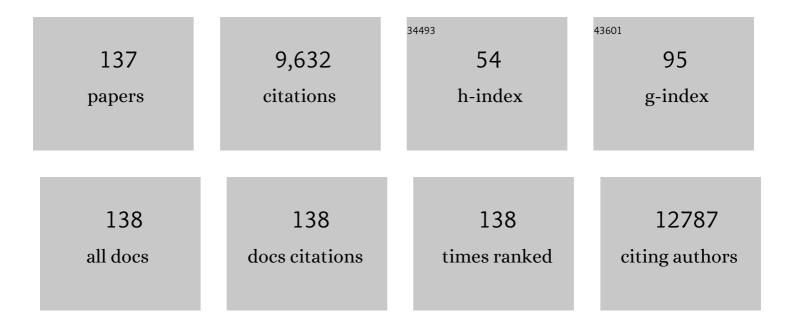
## Yong-Mook Kang

List of Publications by Year in descending order

Source: https://exaly.com/author-pdf/5672434/publications.pdf Version: 2024-02-01



#	Article	IF	CITATIONS
1	Unidirectional electron transport from graphitic-C3N4 for novel remote and long-term photocatalytic anti-corrosion on Q235 carbon steel. Chemical Engineering Journal, 2022, 429, 132520.	6.6	15
2	Steric modulation of Na2Ti2O3(SiO4)·2H2O toward highly reversible Na ion intercalation/deintercalation for Na ion batteries. Chemical Engineering Journal, 2022, 431, 133245.	6.6	3
3	In Situ Defect Engineering Route to Optimize the Cationic Redox Activity of Layered Double Hydroxide Nanosheet via Strong Electronic Coupling with Holey Substrate. Advanced Science, 2022, 9, e2103368.	5.6	19
4	Unraveling vacancy-induced oxygen redox reaction and structural stability in Na-based layered oxides. Chemical Engineering Journal, 2022, 431, 133962.	6.6	11
5	Battery technology and sustainable energy storage and conversion as a new energy resource replacing fossil fuels. , 2022, 1, .		10
6	Regulating Pseudo-Jahn–Teller Effect and Superstructure in Layered Cathode Materials for Reversible Alkali-Ion Intercalation. Journal of the American Chemical Society, 2022, 144, 7929-7938.	6.6	22
7	Effectiveness of salification against shuttle effect in p-type organic batteries: Case studies of triflimide and iodide salts of N,N'-dimethylphenazine. Chemical Engineering Journal, 2022, 446, 137292.	6.6	5
8	Origin of enhanced reversible Na ion storage in hard carbon anodes through p-type molecular doping. Journal of Materials Chemistry A, 2022, 10, 16506-16513.	5.2	5
9	Utilizing Oxygen Redox in Layered Cathode Materials from Multiscale Perspective. Advanced Energy Materials, 2021, 11, 2003227.	10.2	39
10	Structural Engineering of Covalent Organic Frameworks for Rechargeable Batteries. Advanced Energy Materials, 2021, 11, 2003054.	10.2	61
11	Tuning local chemistry of P2 layered-oxide cathode for high energy and long cycles of sodium-ion battery. Nature Communications, 2021, 12, 2256.	5.8	183
12	Direct Cation–Cation Interactions Induced by Mg Dopants for Electron–Gas Behavior in α-Fe <sub>2</sub> O <sub>3</sub> . Journal of Physical Chemistry C, 2021, 125, 12893-12902.	1.5	5
13	Electrochemical grinding-induced metallic assembly exploiting a facile conversion reaction route of metal oxides toward Li ions. Acta Materialia, 2021, 211, 116863.	3.8	12
14	Microstructural Investigation into Na-Ion Storage Behaviors of Cellulose-Based Hard Carbons for Na-Ion Batteries. Journal of Physical Chemistry C, 2021, 125, 14559-14566.	1.5	15
15	Oxygen-Deficient P2-Na <sub>0.7</sub> Mn <sub>0.75</sub> Ni <sub>0.25</sub> O <sub>2â^'<i>x</i></sub> Cathode by a Reductive NH <sub>4</sub> HF <sub>2</sub> Treatment for Highly Reversible Na-Ion Storage. ACS Applied Energy Materials, 2021, 4, 8036-8044.	2.5	15
16	Leading Future Technologies of Energy and Material Science at the College of Engineering, Korea University. Advanced Energy Materials, 2021, 11, 2101200.	10.2	0
17	Two-Phase Transition Induced Amorphous Metal Phosphides Enabling Rapid, Reversible Alkali-Metal Ion Storage. ACS Nano, 2021, 15, 13486-13494.	7.3	23
18	Development of a highly active Fe N C catalyst with the preferential formation of atomic iron sites for oxygen reduction in alkaline and acidic electrolytes. Journal of Colloid and Interface Science, 2021, 596, 148-157.	5.0	13

#	Article	IF	CITATIONS
19	Synergistic Catalysis of the Lattice Oxygen and Transition Metal Facilitating ORR and OER in Perovskite Catalysts for Li–O <sub>2</sub> Batteries. ACS Catalysis, 2021, 11, 424-434.	5.5	72
20	Spinel/Post-spinel engineering on layered oxide cathodes for sodium-ion batteries. EScience, 2021, 1, 13-27.	25.0	194
21	Thermally Activated P2â€O3 Mixed Layered Cathodes toward Synergistic Electrochemical Enhancement for Na Ion Batteries. Advanced Energy Materials, 2021, 11, 2102444.	10.2	17
22	Activating a Multielectron Reaction of NASICON-Structured Cathodes toward High Energy Density for Sodium-Ion Batteries. Journal of the American Chemical Society, 2021, 143, 18091-18102.	6.6	96
23	Elucidating the charge storage mechanism of carbonaceous and organic electrode materials for sodium ion batteries. Chemical Communications, 2021, 57, 13465-13494.	2.2	9
24	Kathodenmaterialien für wiederaufladbare Lithiumbatterien. Angewandte Chemie, 2020, 132, 2598-2626.	1.6	21
25	Advances in the Cathode Materials for Lithium Rechargeable Batteries. Angewandte Chemie - International Edition, 2020, 59, 2578-2605.	7.2	357
26	Crucial roles of interfacial coupling and oxygen defect in multifunctional 2D inorganic nanosheets. Nano Energy, 2020, 67, 104192.	8.2	35
27	Synergistic Control of Structural Disorder and Surface Bonding Nature to Optimize the Functionality of Manganese Oxide as an Electrocatalyst and a Cathode for Li–O 2 Batteries. Small, 2020, 16, 1903265.	5.2	26
28	New Barium Vanadate Ba <i><sub>x</sub></i> V <sub>2</sub> O <sub>5</sub> ( <i>x</i> â‰^ 0.16) for Fast Lithium Intercalation: Lower Symmetry for Higher Flexibility and Electrochemical Durability. Small Methods, 2020, 4, 1900585.	4.6	11
29	Uncovering the Shuttle Effect in Organic Batteries and Counterâ€Strategies Thereof: A Case Study of the <i>N</i> , <i>N′</i> â€Dimethylphenazine Cathode. Angewandte Chemie, 2020, 132, 4052-4063.	1.6	8
30	Largeâ€Scale Synthesis of MOFâ€Derived Superporous Carbon Aerogels with Extraordinary Adsorption Capacity for Organic Solvents. Angewandte Chemie, 2020, 132, 2082-2086.	1.6	70
31	Uncovering the Shuttle Effect in Organic Batteries and Counterâ€Strategies Thereof: A Case Study of the <i>N</i> Nâ€2â€Dimethylphenazine Cathode. Angewandte Chemie - International Edition, 2020, 59, 4023-4034.	7.2	34
32	Largeâ€Scale Synthesis of MOFâ€Derived Superporous Carbon Aerogels with Extraordinary Adsorption Capacity for Organic Solvents. Angewandte Chemie - International Edition, 2020, 59, 2066-2070.	7.2	191
33	Engineering Solid Electrolyte Interphase on Red Phosphorus for Long-Term and High-Capacity Sodium Storage. Chemistry of Materials, 2020, 32, 448-458.	3.2	29
34	Multifunctionalities of Graphene for Exploiting a Facile Conversion Reaction Route of Perovskite CoSnO <sub>3</sub> for Highly Reversible Na Ion Storage. Journal of Physical Chemistry Letters, 2020, 11, 7988-7995.	2.1	5
35	Electrocatalysts: Synergistic Control of Structural Disorder and Surface Bonding Nature to Optimize the Functionality of Manganese Oxide as an Electrocatalyst and a Cathode for Li–O <sub>2</sub> Batteries (Small 12/2020). Small, 2020, 16, 2070062.	5.2	1
36	The origin of heavy element doping to relieve the lattice thermal vibration of layered materials for high energy density Li ion cathodes. Journal of Materials Chemistry A, 2020, 8, 12424-12435.	5.2	37

#	Article	IF	CITATIONS
37	Mesoporous Iron-doped MoS <sub>2</sub> /CoMo <sub>2</sub> S <sub>4</sub> Heterostructures through Organic–Metal Cooperative Interactions on Spherical Micelles for Electrochemical Water Splitting. ACS Nano, 2020, 14, 4141-4152.	7.3	156
38	Phosphorylated polymer/anionic surfactant doped polypyrrole in waterborne epoxy matrix toward enhanced mechanical and chemical resistance. Progress in Organic Coatings, 2020, 143, 105634.	1.9	4
39	Universal Access to Twoâ€Dimensional Mesoporous Heterostructures by Micelleâ€Directed Interfacial Assembly. Angewandte Chemie, 2020, 132, 19738-19743.	1.6	18
40	Universal Access to Twoâ€Dimensional Mesoporous Heterostructures by Micelleâ€Directed Interfacial Assembly. Angewandte Chemie - International Edition, 2020, 59, 19570-19575.	7.2	52
41	Reversible Anionic Redox Activities in Conventional LiNi <sub>1/3</sub> Co <sub>1/3</sub> Mn <sub>1/3</sub> O <sub>2</sub> Cathodes. Angewandte Chemie, 2020, 132, 8759-8766.	1.6	15
42	Tunable Magnetic Exchange between Rare-Earth Metal 5d and Iron 3d States: A Case Study of the Multiple Magnetic Transitions in Gd <sub>6</sub> FeBi <sub>2</sub> and the Solid Solutions Dy <sub>6–<i>x</i></sub> Gd <i><sub>x</sub>/i&gt;FeBi<sub>2</sub> (1 ≤i&gt;x</i> ≤5) with Curie Temperatures in the Range 120–350 K. Chemistry of Materials, 2020, 32, 3087-3096.	3.2	4
43	Regulating the Catalytic Dynamics Through a Crystal Structure Modulation of Bimetallic Catalyst. Advanced Energy Materials, 2020, 10, 1903225.	10.2	21
44	Reversible Anionic Redox Activities in Conventional LiNi <sub>1/3</sub> Co <sub>1/3</sub> Mn <sub>1/3</sub> O <sub>2</sub> Cathodes. Angewandte Chemie - International Edition, 2020, 59, 8681-8688.	7.2	91
45	Interface-Controlled Rhombohedral Li3V2(PO4)3 Embedded in Carbon Nanofibers with Ultrafast Kinetics for Li-Ion Batteries. Journal of Physical Chemistry Letters, 2020, 11, 4059-4069.	2.1	11
46	Highly Reversible and Rapid Sodium Storage in GeP <sub>3</sub> with Synergistic Effect from Outside-In Optimization. ACS Nano, 2020, 14, 4352-4365.	7.3	31
47	Precipitates shape up. Nature Chemistry, 2019, 11, 685-686.	6.6	5
48	Single Atoms for Energy Applications. Small Methods, 2019, 3, 1900523.	4.6	7
49	Triggered reversible phase transformation between layered and spinel structure in manganese-based layered compounds. Nature Communications, 2019, 10, 3385.	5.8	42
50	Rational design and construction of nanoporous iron- and nitrogen-doped carbon electrocatalysts for oxygen reduction reaction. Journal of Materials Chemistry A, 2019, 7, 1380-1393.	5.2	159
51	Controlling the Valence State of Cu Dopant in α-Fe2O3 Anodes: Effects on Crystal Structure and the Conversion Reactions with Alkali Ions. Chemistry of Materials, 2019, 31, 1268-1279.	3.2	23
52	Self-sacrificial templated synthesis of a three-dimensional hierarchical macroporous honeycomb-like ZnO/ZnCo <sub>2</sub> O <sub>4</sub> hybrid for carbon monoxide sensing. Journal of Materials Chemistry A, 2019, 7, 3415-3425.	5.2	66
53	Pseudocapacitive Behavior and Ultrafast Kinetics from Solvated Ion Cointercalation into MoS <sub>2</sub> for Its Alkali Ion Storage. ACS Applied Energy Materials, 2019, 2, 3726-3735.	2.5	9
54	Polydopamine-induced surface functionalization of carbon nanofibers for Pd deposition enabling enhanced catalytic activity for the oxygen reduction and evolution reactions. Journal of Materials Chemistry A, 2019, 7, 7396-7405.	5.2	40

#	Article	IF	CITATIONS
55	Chemical Design of Palladiumâ€Based Nanoarchitectures for Catalytic Applications. Small, 2019, 15, e1804378.	5.2	90
56	Critical design factors for kinetically favorable P-based compounds toward alloying with Na ions for high-power sodium-ion batteries. Energy and Environmental Science, 2019, 12, 1326-1333.	15.6	58
57	<i>In situ</i> self-assembly of Ni <sub>3</sub> S <sub>2</sub> /MnS/CuS/reduced graphene composite on nickel foam for high power supercapacitors. RSC Advances, 2019, 9, 31532-31542.	1.7	18
58	P2/O3 phase-integrated Na0.7MnO2 cathode materials for sodium-ion rechargeable batteries. Journal of Alloys and Compounds, 2019, 771, 987-993.	2.8	45
59	Manganese based layered oxides with modulated electronic and thermodynamic properties for sodium ion batteries. Nature Communications, 2019, 10, 5203.	5.8	202
60	Holey 2D Nanosheets of Lowâ€Valent Manganese Oxides with an Excellent Oxygen Catalytic Activity and a High Functionality as a Catalyst for Li–O <sub>2</sub> Batteries. Advanced Functional Materials, 2018, 28, 1707106.	7.8	61
61	General template-free strategy for fabricating mesoporous two-dimensional mixed oxide nanosheets <i>via</i> self-deconstruction/reconstruction of monodispersed metal glycerate nanospheres. Journal of Materials Chemistry A, 2018, 6, 5971-5983.	5.2	81
62	Spatially Confined Assembly of Monodisperse Ruthenium Nanoclusters in a Hierarchically Ordered Carbon Electrode for Efficient Hydrogen Evolution. Angewandte Chemie, 2018, 130, 5950-5954.	1.6	12
63	Spatially Confined Assembly of Monodisperse Ruthenium Nanoclusters in a Hierarchically Ordered Carbon Electrode for Efficient Hydrogen Evolution. Angewandte Chemie - International Edition, 2018, 57, 5848-5852.	7.2	135
64	Remarkable Enhancement in Sodiumâ€lon Kinetics of NaFe <sub>2</sub> (CN) <sub>6</sub> by Chemical Bonding with Graphene. Small Methods, 2018, 2, 1700346.	4.6	40
65	Bifunctional Conducting Polymer Coated CoP Core–Shell Nanowires on Carbon Paper as a Free‣tanding Anode for Sodium Ion Batteries. Advanced Energy Materials, 2018, 8, 1800283.	10.2	104
66	Recent Developments on and Prospects for Electrode Materials with Hierarchical Structures for Lithiumâ€lon Batteries. Advanced Energy Materials, 2018, 8, 1701415.	10.2	436
67	Frontispiece: αâ€MnO <sub>2</sub> Nanowireâ€Anchored Highly Oxidized Cluster as a Catalyst for Liâ€O <sub>2</sub> Batteries: Superior Electrocatalytic Activity and High Functionality. Angewandte Chemie - International Edition, 2018, 57, .	7.2	1
68	Robust FeCo nanoparticles embedded in a N-doped porous carbon framework for high oxygen conversion catalytic activity in alkaline and acidic media. Journal of Materials Chemistry A, 2018, 6, 23445-23456.	5.2	43
69	Frontispiz: αâ€MnO <sub>2</sub> Nanowireâ€Anchored Highly Oxidized Cluster as a Catalyst for Liâ€O <sub>2</sub> Batteries: Superior Electrocatalytic Activity and High Functionality. Angewandte Chemie, 2018, 130, .	1.6	0
70	αâ€MnO 2 Nanowireâ€Anchored Highly Oxidized Cluster as a Catalyst for Liâ€O 2 Batteries: Superior Electrocatalytic Activity and High Functionality. Angewandte Chemie, 2018, 130, 16216-16221.	1.6	6
71	αâ€MnO <sub>2</sub> Nanowireâ€Anchored Highly Oxidized Cluster as a Catalyst for Liâ€O <sub>2</sub> Batteries: Superior Electrocatalytic Activity and High Functionality. Angewandte Chemie - International Edition, 2018, 57, 15984-15989.	7.2	76
72	All Carbon Dual Ion Batteries. ACS Applied Materials & amp; Interfaces, 2018, 10, 35978-35983.	4.0	93

#	Article	IF	CITATIONS
73	CNT@Ni@Ni–Co silicate core–shell nanocomposite: a synergistic triple-coaxial catalyst for enhancing catalytic activity and controlling side products for Li–O <sub>2</sub> batteries. Journal of Materials Chemistry A, 2018, 6, 10447-10455.	5.2	41
74	GeP3 with soft and tunable bonding nature enabling highly reversible alloying with Na ions. Materials Today Energy, 2018, 9, 126-136.	2.5	31
75	Templateâ€Free Fabrication of Mesoporous Alumina Nanospheres Using Postâ€Synthesis Waterâ€Ethanol Treatment of Monodispersed Aluminium Glycerate Nanospheres for Molybdenum Adsorption. Small, 2018, 14, e1800474.	5.2	50
76	Interlayerâ€5pacingâ€Regulated VOPO <sub>4</sub> Nanosheets with Fast Kinetics for Highâ€Capacity and Durable Rechargeable Magnesium Batteries. Advanced Materials, 2018, 30, e1801984.	11.1	171
77	p â€Phenylenediamine Functionalization Induced 3D Microstructure Formation of Reduced Graphene Oxide for the Improved Electrical double Layer Capacitance in Organic Electrolyte. ChemistrySelect, 2018, 3, 7680-7688.	0.7	13
78	Anisotropic Surface Modulation of Pt Catalysts for Highly Reversible Li–O <sub>2</sub> Batteries: High Index Facet as a Critical Descriptor. ACS Catalysis, 2018, 8, 9006-9015.	5.5	68
79	Oxygen Evolution Reaction: Holey 2D Nanosheets of Low-Valent Manganese Oxides with an Excellent Oxygen Catalytic Activity and a High Functionality as a Catalyst for Li-O2 Batteries (Adv. Funct. Mater.) Tj ETQq1	1 <b>Q</b> 878431	4ogBT /Ove
80	A Glucose-Assisted Hydrothermal Reaction for Directly Transforming Metal–Organic Frameworks into Hollow Carbonaceous Materials. Chemistry of Materials, 2018, 30, 4401-4408.	3.2	102
81	A reduced graphene oxide-encapsulated phosphorus/carbon composite as a promising anode material for high-performance sodium-ion batteries. Journal of Materials Chemistry A, 2017, 5, 3683-3690.	5.2	54
82	Construction of 3D pomegranate-like Na <sub>3</sub> V <sub>2</sub> (PO <sub>4</sub> ) <sub>3</sub> /conducting carbon composites for high-power sodium-ion batteries. Journal of Materials Chemistry A, 2017, 5, 9833-9841.	5.2	101
83	Carbon Nanofibers Heavy Laden with Li <sub>3</sub> V <sub>2</sub> (PO <sub>4</sub> ) <sub>3</sub> Particles Featuring Superb Kinetics for Highâ€Power Lithium Ion Battery. Advanced Science, 2017, 4, 1700128.	5.6	46
84	Investigation of Promising Air Electrode for Realizing Ultimate Lithium Oxygen Battery. Advanced Energy Materials, 2017, 7, 1700234.	10.2	44
85	The synergistic effect of nitrogen doping and para-phenylenediamine functionalization on the physicochemical properties of reduced graphene oxide for electric double layer supercapacitors in organic electrolytes. Journal of Materials Chemistry A, 2017, 5, 12426-12434.	5.2	30
86	Mn-Based Cathode with Synergetic Layered-Tunnel Hybrid Structures and Their Enhanced Electrochemical Performance in Sodium Ion Batteries. ACS Applied Materials & Interfaces, 2017, 9, 21267-21275.	4.0	60
87	Structural and chemical synergistic effect of CoS nanoparticles and porous carbon nanorods for high-performance sodium storage. Nano Energy, 2017, 35, 281-289.	8.2	247
88	Honeycomb-layer structured Na <sub>3</sub> Ni <sub>2</sub> BiO <sub>6</sub> as a high voltage and long life cathode material for sodium-ion batteries. Journal of Materials Chemistry A, 2017, 5, 1300-1310.	5.2	67
89	Pd-Impregnated NiCo <sub>2</sub> O <sub>4</sub> nanosheets/porous carbon composites as a free-standing and binder-free catalyst for a high energy lithium–oxygen battery. Journal of Materials Chemistry A, 2017, 5, 22234-22241.	5.2	49
90	Highâ€Energyâ€Density Metal–Oxygen Batteries: Lithium–Oxygen Batteries vs Sodium–Oxygen Batteries. Advanced Materials, 2017, 29, 1606572.	11.1	138

#	Article	IF	CITATIONS
91	Cobalt phosphide nanoparticles embedded in nitrogen-doped carbon nanosheets: Promising anode material with high rate capability and long cycle life for sodium-ion batteries. Nano Research, 2017, 10, 4337-4350.	5.8	97
92	Shape-controlled synthesis of hierarchically layered lithium transition-metal oxide cathode materials by shear exfoliation in continuous stirred-tank reactors. Journal of Materials Chemistry A, 2017, 5, 25391-25400.	5.2	67
93	Ordered Mesoporous Cobalt Phosphate with Crystallized Walls toward Highly Active Water Oxidation Electrocatalysts. Small, 2016, 12, 1709-1715.	5.2	153
94	Graphiteâ€Nanoplateâ€Coated Bi <sub>2</sub> S <sub>3</sub> Composite with Highâ€Volume Energy Density and Excellent Cycle Life for Roomâ€Temperature Sodium–Sulfide Batteries. Chemistry - A European Journal, 2016, 22, 590-597.	1.7	48
95	Understanding Performance Differences from Various Synthesis Methods: A Case Study of Spinel LiCr <sub>0.2</sub> Ni <sub>0.4</sub> Mn <sub>1.4</sub> O <sub>4</sub> Cathode Material. ACS Applied Materials & Interfaces, 2016, 8, 26051-26057.	4.0	12
96	Urchinâ€Like CoSe <sub>2</sub> as a Highâ€Performance Anode Material for Sodiumâ€lon Batteries. Advanced Functional Materials, 2016, 26, 6728-6735.	7.8	471
97	Carbon oated Si Nanoparticles Anchored between Reduced Graphene Oxides as an Extremely Reversible Anode Material for High Energyâ€Đensity Liâ€Ion Battery. Advanced Energy Materials, 2016, 6, 1600904.	10.2	256
98	Effects of Carbon Content on the Electrochemical Performances of MoS <sub>2</sub> –C Nanocomposites for Li-Ion Batteries. ACS Applied Materials & Interfaces, 2016, 8, 22168-22174.	4.0	46
99	Cobaltâ€Doped FeS <sub>2</sub> Nanospheres with Complete Solid Solubility as a Highâ€Performance Anode Material for Sodiumâ€Ion Batteries. Angewandte Chemie - International Edition, 2016, 55, 12822-12826.	7.2	394
100	Cobaltâ€Doped FeS <sub>2</sub> Nanospheres with Complete Solid Solubility as a Highâ€Performance Anode Material for Sodiumâ€Ion Batteries. Angewandte Chemie, 2016, 128, 13014-13018.	1.6	268
101	Recent Developments of the Lithium Metal Anode for Rechargeable Nonâ€Aqueous Batteries. Advanced Energy Materials, 2016, 6, 1600811.	10.2	306
102	In situ analyses for ion storage materials. Chemical Society Reviews, 2016, 45, 5717-5770.	18.7	101
103	Chemically Bonded Sn Nanoparticles Using the Crosslinked Epoxy Binder for High Energyâ€Đensity Li Ion Battery. Advanced Materials Interfaces, 2016, 3, 1600662.	1.9	17
104	Large size nitrogen-doped graphene-coated graphite for high performance lithium-ion battery anode. RSC Advances, 2016, 6, 104010-104015.	1.7	14
105	A Layerâ€Structured Electrode Material Reformed by a PO <sub>4</sub> â€O <sub>2</sub> Hybrid Framework toward Enhanced Lithium Storage and Stability. Advanced Energy Materials, 2016, 6, 1501717.	10.2	43
106	Elucidation of optoelectronic properties of the sol-gel-grown Al-doped ZnO nanostructures. Journal of Sol-Gel Science and Technology, 2016, 77, 642-649.	1.1	1
107	Fe3O4 nanoparticles encapsulated in one-dimensional Li4Ti5O12 nanomatrix: An extremely reversible anode for long life and high capacity Li-ion batteries. Nano Energy, 2016, 19, 246-256.	8.2	28
108	Controlling Solid-Electrolyte-Interphase Layer by Coating P-Type Semiconductor NiO <sub><i>x</i></sub> on Li <sub>4</sub> Ti <sub>5</sub> O <sub>12</sub> for High-Energy-Density Lithium-Ion Batteries. ACS Applied Materials & Interfaces, 2015, 7, 27934-27939.	4.0	26

#	Article	IF	CITATIONS
109	A Review of the Design Strategies for Tailored Cathode Catalyst Materials in Rechargeable Liâ€O <sub>2</sub> Batteries. Israel Journal of Chemistry, 2015, 55, 458-471.	1.0	22
110	Morphology and Active-Site Engineering for Stable Round-Trip Efficiency Li–O <sub>2</sub> Batteries: A Search for the Most Active Catalytic Site in Co <sub>3</sub> O <sub>4</sub> . ACS Catalysis, 2015, 5, 5116-5122.	5.5	99
111	Facile Method To Synthesize Na-Enriched Na <sub>1+<i>x</i></sub> FeFe(CN) <sub>6</sub> Frameworks as Cathode with Superior Electrochemical Performance for Sodium-Ion Batteries. Chemistry of Materials, 2015, 27, 1997-2003.	3.2	163
112	Critical Descriptor for the Rational Design of Oxide-Based Catalysts in Rechargeable Li–O <sub>2</sub> Batteries: Surface Oxygen Density. Chemistry of Materials, 2015, 27, 3243-3249.	3.2	55
113	Achieving outstanding Li + -ORR and -OER activities via edge- and corner-embedded bimetallic nanocubes for rechargeable Li–O 2 batteries. Nano Energy, 2015, 18, 71-80.	8.2	28
114	An improved catalytic effect of nitrogen-doped TiO <sub>2</sub> nanofibers for rechargeable Li–O <sub>2</sub> batteries; the role of oxidation states and vacancies on the surface. Journal of Materials Chemistry A, 2015, 3, 22557-22563.	5.2	52
115	Na <sub>3</sub> V <sub>2</sub> (PO <sub>4</sub> ) <sub>3</sub> particles partly embedded in carbon nanofibers with superb kinetics for ultra-high power sodium ion batteries. Journal of Materials Chemistry A, 2015, 3, 1005-1009.	5.2	92
116	Polymorphism-induced catalysis difference of TiO <sub>2</sub> nanofibers for rechargeable Li–O <sub>2</sub> batteries. Journal of Materials Chemistry A, 2014, 2, 19660-19664.	5.2	32
117	Enhanced high-temperature cycling of Li2O–2B2O3-coated spinel-structured LiNi0.5Mn1.5O4 cathode material for application to lithium-ion batteries. Journal of Alloys and Compounds, 2014, 601, 217-222.	2.8	45
118	Rapid and controllable synthesis of nitrogen doped reduced graphene oxide using microwave-assisted hydrothermal reaction for high power-density supercapacitors. Carbon, 2014, 73, 106-113.	5.4	105
119	Lithiumâ€lon Transport through a Tailored Disordered Phase on the LiNi <sub>0.5</sub> Mn <sub>1.5</sub> O <sub>4</sub> Surface for Highâ€Power Cathode Materials. ChemSusChem, 2014, 7, 2248-2254.	3.6	25
120	Tailored Oxygen Framework of Li <sub>4</sub> Ti <sub>5</sub> O <sub>12</sub> Nanorods for High-Power Li Ion Battery. Journal of Physical Chemistry Letters, 2014, 5, 1368-1373.	2.1	86
121	Ultra-low overpotential and high rate capability in Li–O2 batteries through surface atom arrangement of PdCu nanocatalysts. Energy and Environmental Science, 2014, 7, 1362.	15.6	193
122	Facile Lithium Ion Transport through Superionic Pathways Formed on the Surface of Li <sub>3</sub> V <sub>2</sub> (PO <sub>4</sub> ) <sub>3</sub> /C for High Power Li Ion Battery. Chemistry of Materials, 2014, 26, 3644-3650.	3.2	68
123	α-MnO2 nanowire catalysts with ultra-high capacity and extremely low overpotential in lithium–air batteries through tailored surface arrangement. Physical Chemistry Chemical Physics, 2013, 15, 20075.	1.3	77
124	β-FeOOH nanorod bundles with highly enhanced round-trip efficiency and extremely low overpotential for lithium-air batteries. Nanoscale, 2013, 5, 11845.	2.8	57
125	[100] Directed Cu-doped h-CoO nanorods: elucidation of the growth mechanism and application to lithium-ion batteries. Nanoscale, 2012, 4, 473-477.	2.8	31
126	Comprehensive design of carbon-encapsulated Fe <sub>3</sub> O <sub>4</sub> nanocrystals and their lithium storage properties. Nanotechnology, 2012, 23, 505401.	1.3	80

#	Article	IF	CITATIONS
127	Kinetics-driven high power Li-ion battery with a-Si/NiSi <inf>x</inf> core-shell nanowire anodes. , 2011, , .		0
128	Kinetics-driven high power Li-ion battery with a-Si/NiSix core-shell nanowire anodes. Chemical Science, 2011, 2, 1090.	3.7	60
129	Structurally stabilized olivine lithium phosphate cathodes with enhanced electrochemical properties through Fe doping. Energy and Environmental Science, 2011, 4, 4978.	15.6	59
130	Nanoengineered Superconducting Wire: Tailored Materials for Highâ€Performance MgB <sub>2</sub> Wire (Adv. Mater. 42/2011). Advanced Materials, 2011, 23, 4820-4820.	11.1	0
131	Syntheses and Characterization of Wurtzite CoO, Rocksalt CoO, and Spinel Co <sub>3</sub> O <sub>4</sub> Nanocrystals: Their Interconversion and Tuning of Phase and Morphology. Chemistry of Materials, 2010, 22, 4446-4454.	3.2	149
132	Maximum Li storage in Si nanowires for the high capacity three-dimensional Li-ion battery. Applied Physics Letters, 2010, 96, .	1.5	147
133	First-Principle Calculation-Assisted Structural Study on the Nanoscale Phase Transition of Si for Li-Ion Secondary Batteries. Inorganic Chemistry, 2009, 48, 11631-11635.	1.9	24
134	Nature of Insulating-Phase Transition and Degradation of Structure and Electrochemical Reactivity in an Olivine-Structured Material, LiFePO <sub>4</sub> . Inorganic Chemistry, 2009, 48, 8271-8275.	1.9	27
135	A study on the charge–discharge mechanism of Co3O4 as an anode for the Li ion secondary battery. Electrochimica Acta, 2005, 50, 3667-3673.	2.6	255
136	Malonic acid assisted sol-gel synthesis and characterization of chromium doped LiMn2O4 spinel. Ionics, 2003, 9, 266-273.	1.2	3
137	Crystallization of lithium cobalt oxide thin films by radio-frequency plasma irradiation. Journal of Applied Physics, 2001, 90, 5940-5945.	1.1	13